TECHNISCHE MECHANIK, Band 28, Heft 3-4, (2008), 185 - 193
Manuskripteingang: 16. Oktober 2007

# A Robust Adaptive Sliding Mode Controller for Remotely Operated Vehicles

Nguyen Quang Hoang, E. Kreuzer

*In order to apply the sliding mode control to a remotely operated vehicle (ROV), prior knowledge of exact bounds for parameter uncertainties and external disturbances is a prerequisite. However, these bounds may not be easily obtained because of the complexity and unpredictability of the structure of uncertainties in the dynamics of ROVs. In order to overcome such a difficulty in the control of ROVs, we propose a new robust adaptive sliding mode for dynamic positioning and trajectory tracking of ROVs. By applying this adaptive sliding mode controller, prior knowledge is not required because the controller is able to estimate the bounds of uncertainties and external disturbances. The stability of the control algorithm can be easily verified by using Lyapunov theory. The effectiveness of this design control method is demonstrated by means of numerical experiments.*

## 1 Introduction

Applications of remotely operated vehicles have extensively grown in the last twenty years both for scientific investigations and industrial needs. ROVs play an important role not only in offshore oil operations but also in a number of other applications, such as fisheries research, dam inspection, salvage operations, military applications, etc., wherever human diver interventions are risky or impossible, Goheen, K.G. and Jefferys, E.R. (1990).

Making a ROV a reality, however, one faces significant challenges, notably difficulties in designing the control system of a ROV. The control of ROVs confronts a number of unique and demanding problems. Major facts that make it difficult to control ROVs include, inter alia: the highly nonlinear, time-varying dynamic behavior of the vehicle; uncertainties in hydrodynamics coefficients; the higher order and redundant structure when a manipulator is attached; disturbances by ocean currents; and changes in the center of the gravity and buoyancy due to the manipulator motion which simultaneously disturbs the vehicle.

So far sliding mode control is widely applied in the control of ROVs thanks to its simplicity and robustness properties, Slotine, J.J.E. (1991). Sliding mode control is a control technique which has many attractive features: besides robustness to parameter variations its insensitivity to disturbances, Khalil, H.K. (1996), has to be mentioned. This type of control has been known as a useful strategy to apply to uncertain systems. When the state is constrained to the sliding surface, sliding mode control can completely reject uncertainties which satisfy the matching condition, Utkin, V. (1978). In sliding mode control a vital assumption is that the uncertainties are bounded and their bounds are available to the designers. These bounds are an important clue to the possibility of guaranteed stability of a closed loop system. Unfortunately, due to the complexity of the structure of uncertainties in the dynamics of ROVs, such bounds may not be easily obtained.

Sliding mode control has been applied quite successfully in the control of underwater vehicles by Yoerger and Slotine, Yoerger, D. R. and Slotine, J. E. (1985). They proposed to use a series of single-input single-output (SISO) continuous time controller. They investigated the effects of uncertainties of the hydrodynamic coefficients and neglecting cross-coupling terms. Cristi *et al.*, Cristi, R.; Papoulias, F. A.; and Healey, A. J. (1990) employed an adaptive sliding mode controller to control an underwater vehicle in the dive plane. In their work, they developed the control law based on a linear model which assumed no information regarding nonlinear characteristics of the vehicle dynamics. Walchko *et al.*, Walchko, K.J.; Novick, D.; and Nechyba, M.C. (2003) applied sliding mode to control a ROV named Subjugator. In Walchko's study the coriolis and centrifugal terms in the dynamic model of the ROV are neglected.

However, what all these studies have in common is that the availabilities of bounds for uncertainties must be

given in advance to the designers of ROVs. It therefore confronts with the problem in obtaining the bounds of uncertainties in control of ROVs as described above.

In order to cope with this problem, this study presents a new robust adaptive sliding mode for dynamic positioning and trajectory tracking of a ROV. By applying this adaptive sliding mode controller, prior knowledge of exact bounds for parameter uncertainties and external disturbances is not needed because the controller is able to estimate the bound of uncertainties and external disturbances. The stability of control algorithm can be easily verified by using Lyapunov theory. The effectiveness of this design control method is demonstrated by means of numerical experiments. Unfortunately, sliding mode also has other limitations, namely control chattering and robustness only to matched uncertainties. The chattering drawback of sliding mode controller is caused by imperfections in switching devices and delays. Chattering results in low control accuracy, high heat losses in electrical power circuits, high wear of moving mechanical parts. It may also excite unmodeled high-frequency dynamics, which degrades the performance of the system and may even lead to instability. One approach to eliminate chattering is to use a continuous approximation of the discontinuous sliding mode controller, Kreuzer, E. and Pinto, F.C. (1996); Pinto, F. (1996); Slotine, J.J.E. (1991). In this study, we also apply this approach to overcome this drawback.

## 2 Dynamic Model of ROV

The kinetics of an underwater vehicle can be described in a common way through six degrees of freedom (DOF) by means of two coordinate frames, a body-fixed frame and an earth-fixed frame, Figure 1. In general, the mathematical model of underwater vehicles can be represented by the following vector equation, Fossen, T.I. (1994)

$$\begin{aligned} \boldsymbol{M}\dot{\boldsymbol{\nu}} + \boldsymbol{C}(\boldsymbol{\nu})\boldsymbol{\nu} + \boldsymbol{D}(\boldsymbol{\nu})\boldsymbol{\nu} + \boldsymbol{g}(\boldsymbol{\eta}) + \boldsymbol{d}_v &= \boldsymbol{\tau}_v \\ \dot{\boldsymbol{\eta}} &= \boldsymbol{J}(\boldsymbol{\eta}_2)\boldsymbol{\nu} \end{aligned} \tag{1}$$

where $\boldsymbol{\eta} = [x,\ y,\ z,\ \phi,\ \theta,\ \psi]^T$ is the position and attitude vector with respect to the earth-fixed reference frame, $\boldsymbol{\nu} = [u,\ v, w,\ p,\ q,\ r]^T$ is the vector of linear velocity and angular velocity with respect to the body-fixed frame, $\boldsymbol{M}$ is a constant positive definite and symmetric inertia matrix (which includes the added inertia), $\boldsymbol{C}(\boldsymbol{\nu})$ is a skew-symmetric matrix linear in $\boldsymbol{\nu}$ containing the Coriolis and centripetal terms, $\boldsymbol{D}(\boldsymbol{\nu})$ is a positive definite damping matrix containing drag and lift terms (and possibly skin friction and viscous damping), and $\boldsymbol{g}(\boldsymbol{\eta})$ is the vector of restoring forces/moments (gravitational and buoyant forces/moments), $\boldsymbol{J}(\boldsymbol{\eta})$ is the transformation matrix between body-fixed and earth-fixed frame and $\boldsymbol{d}_v$ summarizes the environmental disturbances and disturbances due to a tether cable. The wave-induced forces/moments are assumed negligible since the vehicle operates below the wave-affected zone, the operating depth is normally significantly greater than 20 m. The variations of water density are also considered to be negligible.

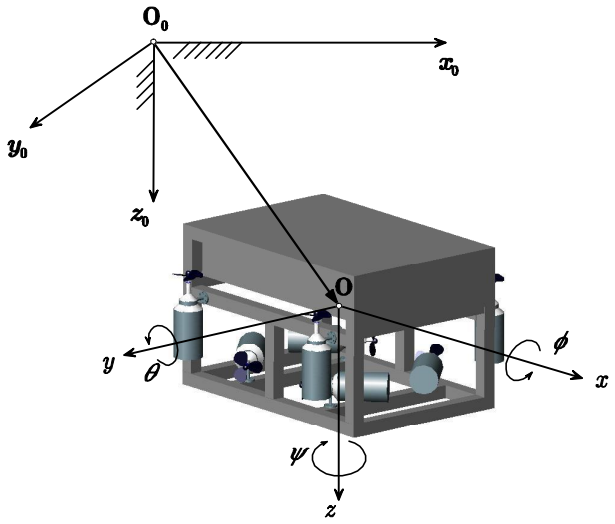


Figure 1: ROV model with two coordinate systems

**Hydrodynamic Forces**

As the vehicle moves underwater, additional forces and moments coefficients are added to account for the effective mass of the fluid that surrounds the vehicle and must be accelerated with the vehicle. To describe the interaction between fluid and ROV the Morison's equation will be used, Newman, J.N. (1982)

$$\boldsymbol{F}_h = \tfrac{1}{2} C_d \rho_W A |\boldsymbol{\nu}| \boldsymbol{\nu} + C_m \rho_W V_W \dot{\boldsymbol{\nu}} + \rho_W V_W \dot{\boldsymbol{\nu}}_W \tag{2}$$

where $A$ represents a reference area of the ROV; $\rho_W$ is the density of the water; $C_m$ is the added mass coefficient; $V_W$ is the water volume displaced by the vehicle; $\boldsymbol{\nu}$ and $\dot{\boldsymbol{\nu}}$ are the relative velocity and the relative acceleration between vehicle and water, respectively. The acceleration $\dot{\boldsymbol{\nu}}_W$ of the water itself can in general be neglected at normal working depths and so the last term in equation (2) vanishes. Moreover, the relative acceleration turns into the acceleration of the vehicle itself. The factor $C_m \rho_W V_W$ can then be included in the inertia matrix $\boldsymbol{M}$ as the *added masses*. The damping due to the ROV motion in the fluid is expressed by the coefficient $C_d$ and has a non-linear character due to the term $|\boldsymbol{\nu}|\boldsymbol{\nu}$. The damping is taken into account in $\boldsymbol{D}(\boldsymbol{\nu})$, that is a real and strictly positive matrix, with rough assumptions such as a symmetric vehicle and non-coupled motion. It can be simplified to a diagonal matrix $\boldsymbol{D}(\boldsymbol{\nu}) = diag(d_1|u|,\ d_2|v|,\ d_3|w|,\ d_4|p|,\ d_5|q|,\ d_6|r|)$ where $d_i$ ($i$ = 1, 2, ..., 6) is the drag coefficient, here the linear damping is negligible. Both $C_d$ and $C_m$ are also difficult to determine theoretically and may be obtained through measurements. They depend in general on the geometry of the vehicle and also on the direction of relative velocity of the ROV.

**Thruster Forces**

The thruster forces $\boldsymbol{u}$ are the output vector of the thruster system the dynamics of which are nonlinear and quite complex. Moreover, the relationship between the force/moment acting on the vehicle $\boldsymbol{\tau}_v$ and the propulsion of the propellers $\boldsymbol{u}$ also is highly nonlinear. In general, the thruster force and moment vector will be a complicated function depending on the vehicle's velocity vector $\boldsymbol{\nu} \in \mathbb{R}^6$ and the control variable $\boldsymbol{n} \in \mathbb{R}^p$, which contains the angular velocities of propellers. Here $p$ is the number of control input, e.g. the number of thrusters. A detailed theoretical and experimental analysis of thrusters' behavior can be found in Bachmayer, R. and Whitcomb, L.L. (August 1999); Whitcomb, L.L. and Yoerger, D.R. (1999a,b). Normally, underwater vehicles are driven by brushless DC motors. With the assumption that the time constant of thruster dynamics is much smaller than the time constant of vehicle dynamics, a simple static thruster model is often used. Each thruster force $u_i$ is proportional to $|n_i| n_i$, where $n_i$ is the thruster's propeller angular velocity and proportional to the motor drive voltage $V_m$. A simplified relationship between $\boldsymbol{\tau}_v$ and $\boldsymbol{u}$ is expressed through the linear mapping, Fossen, T.I. (1994)

$$\boldsymbol{\tau}_v = \boldsymbol{B}\boldsymbol{u} \tag{3}$$

where $\boldsymbol{B} \in \mathbb{R}^{6\times p}$ is a known and constant matrix which depends on the configuration of thrusters on the vehicle, $\boldsymbol{B}\boldsymbol{B}^{\mathrm{T}}$ is non-singular, *T* here means the transposition of a matrix or a vector, and $\boldsymbol{u}$ is the vector the components of which are thruster forces. The ROV dynamics (1) can be also written in earth-fixed coordinates as follows

$$\boldsymbol{M}_\eta(\boldsymbol{\eta})\ddot{\boldsymbol{\eta}} + \boldsymbol{C}_\eta(\boldsymbol{\eta},\dot{\boldsymbol{\eta}})\dot{\boldsymbol{\eta}} + \boldsymbol{D}_\eta(\boldsymbol{\eta},\dot{\boldsymbol{\eta}})\dot{\boldsymbol{\eta}} + \boldsymbol{g}_\eta(\boldsymbol{\eta}) + \boldsymbol{d}_\eta = \boldsymbol{\tau}_\eta \tag{4}$$

where

$$\boldsymbol{M}_\eta(\boldsymbol{\eta}) = \boldsymbol{J}^{-T}(\boldsymbol{\eta})\boldsymbol{M}\boldsymbol{J}^{-1}(\boldsymbol{\eta}), \quad \boldsymbol{C}_\eta(\boldsymbol{\eta},\dot{\boldsymbol{\eta}}) = \boldsymbol{J}^{-T}(\boldsymbol{\eta})[\boldsymbol{C}(\boldsymbol{\nu}) - \boldsymbol{M}\boldsymbol{J}^{-1}(\boldsymbol{\eta})\dot{\boldsymbol{J}}(\boldsymbol{\eta})]\boldsymbol{J}^{-1}(\boldsymbol{\eta})$$
$$\boldsymbol{D}_\eta(\boldsymbol{\eta},\dot{\boldsymbol{\eta}}) = \boldsymbol{J}^{-T}(\boldsymbol{\eta})\boldsymbol{D}(\boldsymbol{\nu})\boldsymbol{J}^{-1}(\boldsymbol{\eta}),\ \boldsymbol{g}_\eta(\boldsymbol{\eta}) = \boldsymbol{J}^{-T}(\boldsymbol{\eta})\boldsymbol{g}(\boldsymbol{\eta}), \quad \boldsymbol{d}_\eta = \boldsymbol{J}^{-T}(\boldsymbol{\eta})\boldsymbol{d}_v.$$

We assume that the underwater vehicle has uncertainties, i.e.

$$\begin{aligned} &\boldsymbol{M}_\eta(\boldsymbol{\eta}) = \boldsymbol{M}_0(\boldsymbol{\eta}) + \Delta\boldsymbol{M}_\eta(\boldsymbol{\eta}), \quad \boldsymbol{C}_\eta(\boldsymbol{\eta},\dot{\boldsymbol{\eta}}) = \boldsymbol{C}_0(\boldsymbol{\eta},\dot{\boldsymbol{\eta}}) + \Delta\boldsymbol{C}_\eta(\boldsymbol{\eta},\dot{\boldsymbol{\eta}}) \\ &\boldsymbol{D}_\eta(\boldsymbol{\eta},\dot{\boldsymbol{\eta}}) = \boldsymbol{D}_0(\boldsymbol{\eta},\dot{\boldsymbol{\eta}}) + \Delta\boldsymbol{D}_\eta(\boldsymbol{\eta},\dot{\boldsymbol{\eta}}), \qquad \boldsymbol{g}_\eta(\boldsymbol{\eta}) = \boldsymbol{g}_0(\boldsymbol{\eta}) + \Delta\boldsymbol{g}_\eta(\boldsymbol{\eta}). \end{aligned} \tag{5}$$

The uncertain components represent bounded, small, possible time varying, unmodelled dynamics or load changes. Substituting the expression (5) into the dynamics (4) gives rise to

$$\boldsymbol{M}_0(\boldsymbol{\eta})\ddot{\boldsymbol{\eta}} + \boldsymbol{C}_0(\boldsymbol{\eta},\dot{\boldsymbol{\eta}})\dot{\boldsymbol{\eta}} + \boldsymbol{D}_0(\boldsymbol{\eta},\dot{\boldsymbol{\eta}})\dot{\boldsymbol{\eta}} + \boldsymbol{g}_0(\boldsymbol{\eta}) + \boldsymbol{\delta} = \boldsymbol{\tau} \tag{6}$$

with

$$\boldsymbol{\tau} = \boldsymbol{J}^{-T}(\boldsymbol{\eta})\boldsymbol{\tau}_v \tag{7}$$

$$\boldsymbol{\delta} = \Delta\boldsymbol{M}(\boldsymbol{\eta})\ddot{\boldsymbol{\eta}} + \Delta\boldsymbol{C}(\boldsymbol{\eta},\dot{\boldsymbol{\eta}})\dot{\boldsymbol{\eta}} + \Delta\boldsymbol{D}(\boldsymbol{\eta},\dot{\boldsymbol{\eta}})\dot{\boldsymbol{\eta}} + \Delta\boldsymbol{g}(\boldsymbol{\eta}) + \boldsymbol{d}_\eta . \tag{8}$$

Here $\boldsymbol{\delta}$ represents all the uncertain terms and environmental disturbances. In the cases $\boldsymbol{\delta} \equiv \boldsymbol{0}$, we call the dynamics the *nominal dynamics* of the underwater vehicle. For this uncertainty, we assume the following boundedness condition. This assumption is usually satisfied in practice.

*Assumption*: There exist positive constants $\rho_0$, $\rho_1$ and $\rho_2$ such that

$$\|\boldsymbol{\delta}\| \le \rho_0 + \rho_1 \|\boldsymbol{e}\| + \rho_2 \|\dot{\boldsymbol{e}}\| \tag{9}$$

where the tracking error vector e is defined as

$$\boldsymbol{e} = \boldsymbol{\eta}(t) - \boldsymbol{\eta}_d(t)$$

with $\boldsymbol{\eta}_d(t)$ is a desired trajectory.

## 3 Sliding Mode Control for ROV

Sliding mode control is a model-based method that uses the equation of motion to anticipate dynamic effects as well as react to feedback errors. It handles the non-linear character of a system, and can naturally deal with the speed dependent effects and multi-axis coupling effects seen in a ROV. A sliding mode controller can be configured to include an adaptive extension to compensate for changes in environment, vehicle buoyancy, etc. In general, the method has also several drawbacks. It requires a good dynamic model of the system and the knowledge of the inaccuracies or uncertainties in the model as well as a full-state feedback. Sliding mode control offers the best combination of performance, analytical performance guarantees, and design ease, Hills, S.J. and Yoerger, D.R. (1994).

In order to design the sliding controller for a multivariable system like an ROV, the sliding surface has to be defined, Berstecher, R. (1998); Gao, W. and Hung, J.C. (1993)

$$\boldsymbol{s} = \dot{\boldsymbol{e}} + \boldsymbol{\lambda}\boldsymbol{e} = \dot{\boldsymbol{\eta}} - \dot{\boldsymbol{\eta}}_r \tag{10}$$

where $\boldsymbol{s} \in R^6$, and $\boldsymbol{\lambda}$ is a positive constant.

As can be seen from (10), maintaining system states on the surface for all $t > 0$ will satisfy the tracking requirements $\boldsymbol{\eta}(t) \to \boldsymbol{\eta}_d(t)$. Indeed, it will force the error vector $\boldsymbol{e}(t)$ to approach zero, given any bounded initial condition $\boldsymbol{e}(0)$.

In order to give out the control force, let's consider a Lyapunov-like function candidate as

$$V(\boldsymbol{s},t) = \frac{1}{2}\boldsymbol{s}^T\boldsymbol{M}_0(\boldsymbol{\eta})\boldsymbol{s} . \tag{11}$$

Differentiating $V(\boldsymbol{s},t)$ with respect to time under consideration of (10) one obtains

$$\dot{V}(\boldsymbol{s},t) = \boldsymbol{s}^T\boldsymbol{M}_0(\boldsymbol{\eta})\dot{\boldsymbol{s}} + \frac{1}{2}\boldsymbol{s}^T\dot{\boldsymbol{M}}_0(\boldsymbol{\eta})\boldsymbol{s} = \boldsymbol{s}^T\boldsymbol{M}_0(\boldsymbol{\eta})(\ddot{\boldsymbol{\eta}} - \ddot{\boldsymbol{\eta}}_r) + \frac{1}{2}\boldsymbol{s}^T\dot{\boldsymbol{M}}_0(\boldsymbol{\eta})\boldsymbol{s} . \tag{12}$$

Substituting $\boldsymbol{M}_0(\boldsymbol{\eta})\ddot{\boldsymbol{\eta}}$ from (4) into (12) yields

$$\dot{V} = \boldsymbol{s}^T\left[\boldsymbol{\tau} - \boldsymbol{C}_0(\boldsymbol{\nu},\boldsymbol{\eta})\dot{\boldsymbol{\eta}} - \boldsymbol{D}_0(\boldsymbol{\nu},\boldsymbol{\eta})\dot{\boldsymbol{\eta}} - \boldsymbol{g}_0(\boldsymbol{\eta}) - \boldsymbol{\delta} - \boldsymbol{M}_0(\boldsymbol{\eta})\ddot{\boldsymbol{\eta}}_r\right] + \frac{1}{2}\boldsymbol{s}^T\dot{\boldsymbol{M}}_0(\boldsymbol{\eta})\boldsymbol{s} , \tag{13}$$

or

$$\dot{V} = \boldsymbol{s}^T\left[\boldsymbol{\tau} - \boldsymbol{C}_0(\boldsymbol{\nu},\boldsymbol{\eta})\dot{\boldsymbol{\eta}}_r - \boldsymbol{D}_0(\boldsymbol{\nu},\boldsymbol{\eta})\dot{\boldsymbol{\eta}} - \boldsymbol{g}_0(\boldsymbol{\eta}) - \boldsymbol{\delta} - \boldsymbol{M}_0(\boldsymbol{\eta})\ddot{\boldsymbol{\eta}}_r\right] \tag{14}$$

noting that in (14) the property of skew-symmetry of matrix $\left[\frac{1}{2}\dot{\boldsymbol{M}}_0(\boldsymbol{\eta}) - \boldsymbol{C}_0(\boldsymbol{\nu},\boldsymbol{\eta})\right]$ has been used.

In order to guarantee $\dot{V} < -\varepsilon\|\boldsymbol{s}\|$, in which $\varepsilon$ is a small positive number, the control force $\boldsymbol{\tau}$ can be chosen

as

$$\boldsymbol{\tau} = \boldsymbol{\tau}_{cont} + \boldsymbol{\tau}_{dis}$$

with

$$\boldsymbol{\tau}_{cont} = \boldsymbol{M}_0(\boldsymbol{\eta})\ddot{\boldsymbol{\eta}}_r + \boldsymbol{C}_0(\boldsymbol{\nu},\boldsymbol{\eta})\dot{\boldsymbol{\eta}}_r + \boldsymbol{D}_0(\boldsymbol{\nu},\boldsymbol{\eta})\dot{\boldsymbol{\eta}} + \boldsymbol{g}_0(\boldsymbol{\eta}) \tag{15}$$

and

$$\boldsymbol{\tau}_{dis} = -\boldsymbol{K}\,\mathrm{sgn}(\boldsymbol{s}), \qquad K_{i,i} > |\delta_i| + \varepsilon\,. \tag{16}$$

By choosing the control force as (15) and (16), the time derivative of $V$ is negative definite and thus $\boldsymbol{s}$ tends to zero asymptotically.

The control law obtaining the *sign* function as in (16) may lead the system to chattering. In order to avoid this phenomenon, we apply the following smoothing control function as used in Kiriazov, P.; Kreuzer, E.; and Pinto, F. (1997) instead of the *sign*-function in (16)

$$\mathrm{sgn}(x) \approx \frac{2}{\pi}\arctan(cx)\,. \tag{17}$$

In (17) the coefficient $c$ should be chosen large enough, so that the two functions are almost the same.

## 4 Adaptive Sliding Mode Control

Applying the sliding mode control for the ROV definitely requires the bounds of uncertainties and disturbances in advance. In the case of underwater vehicles, the complexity and unpredictability of the structure of uncertainties may particularly cause certain difficulties in obtaining these bounds. To overcome such a problem, we propose to apply the adaptive sliding mode control in order to estimate these bounds of uncertainties and external disturbances online. Now, the form of the adaptive sliding mode control is proposed as follows

$$\boldsymbol{\tau} = \boldsymbol{\tau}_{cont} + \boldsymbol{\tau}_{lin} + \boldsymbol{\tau}_{dis} \tag{18}$$

where $\boldsymbol{\tau}_{cont}$ is defined in equation (15) and $\boldsymbol{\tau}_{dis}$ is given in the following as

$$\boldsymbol{\tau}_{dis} = \begin{cases} -(\hat{\rho}_0 + \hat{\rho}_1 \|\boldsymbol{e}\| + \hat{\rho}_2 \|\dot{\boldsymbol{e}}\|)\,\mathrm{sgn}(\boldsymbol{s}), & \|\boldsymbol{s}\| > 0 \\ 0, & \|\boldsymbol{s}\| > 0 \end{cases} \tag{19}$$

where $\hat{\rho}_0$, $\hat{\rho}_1$ and $\hat{\rho}_2$ are the adaptive variables for $\rho_0$, $\rho_1$ and $\rho_2$ defined in equation (9). The linear controller $\boldsymbol{\tau}_{lin}$ is chosen as follows

$$\boldsymbol{\tau}_{lin} = -\boldsymbol{K}_{pd}\boldsymbol{s} \tag{20}$$

with the positive definite matrix $\boldsymbol{K}_{pd}$.

*Theorem*. If the control law (18) with the following adaptation law is applied to the nonlinear uncertain system defined by (4), the overall system is globally asymptotically stable

$$\left.\begin{aligned} \dot{\hat{\rho}}_0 &= -c_0^{-1}\|\boldsymbol{s}\| \\ \dot{\hat{\rho}}_1 &= -c_1^{-1}\|\boldsymbol{s}\|\cdot\|\boldsymbol{e}\| \\ \dot{\hat{\rho}}_2 &= -c_2^{-1}\|\boldsymbol{s}\|\cdot\|\dot{\boldsymbol{e}}\| \end{aligned}\right\} \tag{21}$$

where $c_0$, $c_1$ and $c_2$ are arbitrary positive constants.

*Proof*: Let us consider the following positive definite function as a Lyapunov function candidate

$$V(\boldsymbol{s},t) = \frac{1}{2}\boldsymbol{s}^T\boldsymbol{M}_0(\boldsymbol{\eta})\boldsymbol{s} + \frac{1}{2}\sum_{i=0}^{2} c_i\tilde{\rho}_i^2 \tag{22}$$

where $c_i$ ($i$ = 0, 1, 2) are positive constants, $\tilde{\rho}_i = \hat{\rho}_i - \rho_i$.
Differentiating $V$ with respect to time yields

$$\dot{V}(\boldsymbol{s},t) = \boldsymbol{s}^T \boldsymbol{M}_0(\boldsymbol{\eta})\dot{\boldsymbol{s}} + \frac{1}{2}\boldsymbol{s}^T \dot{\boldsymbol{M}}_0(\boldsymbol{\eta})\boldsymbol{s} + \sum_{i=0}^{2} c_i \tilde{\rho}_i \dot{\tilde{\rho}}_i \,.$$

From (10) we obtain $\dot{\boldsymbol{s}} = \ddot{\boldsymbol{\eta}} - \ddot{\boldsymbol{\eta}}_r$. Hence,

$$\dot{V}(\boldsymbol{s},t) = \boldsymbol{s}^T \boldsymbol{M}_0(\boldsymbol{\eta})[\ddot{\boldsymbol{\eta}} - \ddot{\boldsymbol{\eta}}_r] + \frac{1}{2}\boldsymbol{s}^T \dot{\boldsymbol{M}}_0(\boldsymbol{\eta})\boldsymbol{s} + \sum_{i=0}^{2} c_i \tilde{\rho}_i \dot{\tilde{\rho}}_i$$

with $\boldsymbol{M}_0(\boldsymbol{\eta})\ddot{\boldsymbol{\eta}}$ calculated from (4), we obtain

$$\dot{V} = \boldsymbol{s}^T \left[\boldsymbol{\tau} - \boldsymbol{C}_0(\boldsymbol{\nu},\boldsymbol{\eta})\dot{\boldsymbol{\eta}}_r - \boldsymbol{D}_0(\boldsymbol{\nu},\boldsymbol{\eta})\dot{\boldsymbol{\eta}} - \boldsymbol{g}_0(\boldsymbol{\eta}) - \boldsymbol{\delta} - \boldsymbol{M}_0(\boldsymbol{\eta})\ddot{\boldsymbol{\eta}}_r\right] + \sum_{i=0}^{2} c_i \tilde{\rho}_i \dot{\tilde{\rho}}_i \,. \tag{23}$$

Substituting (18) with (15), (20) and (19) into (23) we obtain

$$\dot{V} = -\boldsymbol{s}^T \boldsymbol{K}_{pd} \boldsymbol{s} + \boldsymbol{s}^T \left[\boldsymbol{\tau}_{dis} - \boldsymbol{\delta}\right] + \sum_{i=0}^{2} c_i \tilde{\rho}_i \dot{\tilde{\rho}}_i \,. \tag{24}$$

With assumption (9), we obtain the following estimations

$$\boldsymbol{s}^T \boldsymbol{\delta} \le \|\boldsymbol{s}\|(\rho_0 + \rho_1 \|\boldsymbol{e}\| + \rho_2 \|\dot{\boldsymbol{e}}\|) = \|\boldsymbol{s}\|(\hat{\rho}_0 + \hat{\rho}_1 \|\boldsymbol{e}\| + \hat{\rho}_2 \|\dot{\boldsymbol{e}}\|) - \|\boldsymbol{s}\|(\tilde{\rho}_0 + \tilde{\rho}_1 \|\boldsymbol{e}\| + \tilde{\rho}_2 \|\dot{\boldsymbol{e}}\|)\,, \tag{25}$$

$$\begin{aligned} \boldsymbol{s}^T \boldsymbol{\tau}_{dis} &= -\boldsymbol{s}^T \operatorname{sgn}(\boldsymbol{s})(\rho_0 + \rho_1 \|\boldsymbol{e}\| + \rho_2 \|\dot{\boldsymbol{e}}\|) \\ &= -\sum_{i=1}^{6} |s_i|(\hat{\rho}_0 + \hat{\rho}_1 \|\boldsymbol{e}\| + \hat{\rho}_2 \|\dot{\boldsymbol{e}}\|) \le -\|\boldsymbol{s}\|(\tilde{\rho}_0 + \tilde{\rho}_1 \|\boldsymbol{e}\| + \tilde{\rho}_2 \|\dot{\boldsymbol{e}}\|). \end{aligned} \tag{26}$$

With (25) and (26), the equation (24) is written

$$\begin{aligned} \dot{V} \le -\boldsymbol{s}^T \boldsymbol{K}\boldsymbol{s} &+ \|\boldsymbol{s}\|(\hat{\rho}_0 + \hat{\rho}_1 \|\boldsymbol{e}\| + \hat{\rho}_2 \|\dot{\boldsymbol{e}}\|) - \|\boldsymbol{s}\|(\hat{\rho}_0 + \hat{\rho}_1 \|\boldsymbol{e}\| + \hat{\rho}_2 \|\dot{\boldsymbol{e}}\|) + \\ &\|\boldsymbol{s}\|(\tilde{\rho}_0 + \tilde{\rho}_1 \|\boldsymbol{e}\| + \tilde{\rho}_2 \|\dot{\boldsymbol{e}}\|) + + \sum_{i=0}^{2} c_i \tilde{\rho}_i \dot{\tilde{\rho}}_i. \\ \dot{V} \le -\boldsymbol{s}^T \boldsymbol{K}\boldsymbol{s} &+ \|\boldsymbol{s}\|(\tilde{\rho}_0 + \tilde{\rho}_1 \|\boldsymbol{e}\| + \tilde{\rho}_2 \|\dot{\boldsymbol{e}}\|) + + \sum_{i=0}^{2} c_i \tilde{\rho}_i \dot{\tilde{\rho}}_i \\ \dot{V} \le -\boldsymbol{s}^T \boldsymbol{K}\boldsymbol{s} &+ (c_0 \dot{\tilde{\rho}}_0 + \|\boldsymbol{s}\|)\tilde{\rho}_0 + (c_1 \dot{\tilde{\rho}}_1 + \|\boldsymbol{s}\| \cdot \|\boldsymbol{e}\|)\tilde{\rho}_1 + (c_2 \dot{\tilde{\rho}}_2 + \|\boldsymbol{s}\| \cdot \|\dot{\boldsymbol{e}}\|)\tilde{\rho}_2 \,. \end{aligned} \tag{27}$$

Substituting (21) into (27) one obtains

$$\dot{V} \le -\boldsymbol{s}^T \boldsymbol{K}\boldsymbol{s} < 0, \qquad \forall \|\boldsymbol{s}\| \ne 0 \,.$$

This completes the proof.

Finally, the control forces/moments $\boldsymbol{\tau}$ defined by (18) are distributed for $p$ thrusters based on least mean square method

$$\boldsymbol{u} = \boldsymbol{B}^T (\boldsymbol{B}\boldsymbol{B}^T)^{-1} \boldsymbol{J}(\boldsymbol{\eta})^T \boldsymbol{\tau} \,. \tag{28}$$

## 5 Numerical Experiments

Aiming to verify the robustness and the reliability of the controller, a dynamic model of an ROV having the geometrical and the mechanical structure of our experimental vehicle is taken for the numerical control design consideration. The experimental ROV developed at the Institute of Mechanics and Ocean Engineering of Hamburg University of Technology is shown in Figure 2. Its dry weight is about 80 *kg*, the ROV is designed so that its buoyancy is slightly larger than its weight. The propulsion system is made of eight marine propellers, which are driven by DC motors. One passive arm with six DOFs is used as a position sensor for the region close to submerged structure.

For the simulation, we assume firstly that the inertial parameters, such as the added masses, are estimated with an accuracy of 20 percent. The difference between drag coefficients of the actual model and the nominal model is less than 20 percent. Besides, the actual model is also disturbed by a harmonic function with a constant part and their parameters were varied.

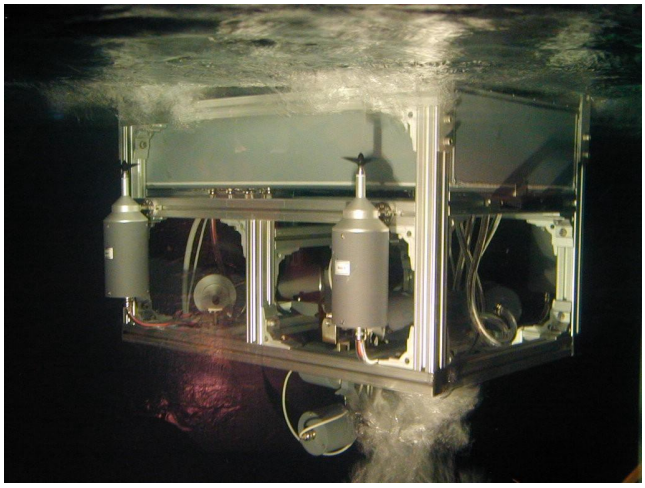

Figure 2: The experimental vehicle

The first numerical experiment is a point-to-point control and station keeping at the endpoint for the vehicles. In this experiment, the ROV moves from point $(x, y, z, \psi) = (0, 0, 0, 0)$ to point $(3, 2.5, 2\,\mathrm{m},\ 1.0\,\mathrm{rad})$ and then stays at this point. The performances of the system are shown in Figures 3 and 4. The results show that the desired position is reached after about 10 seconds.

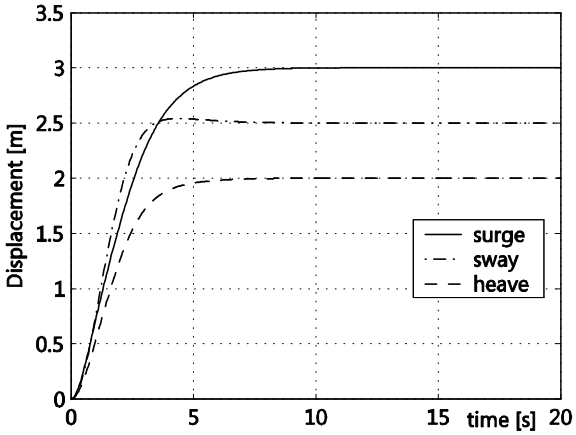


Figure 3: Time history of $x(t)$, $y(t)$ and $z(t)$

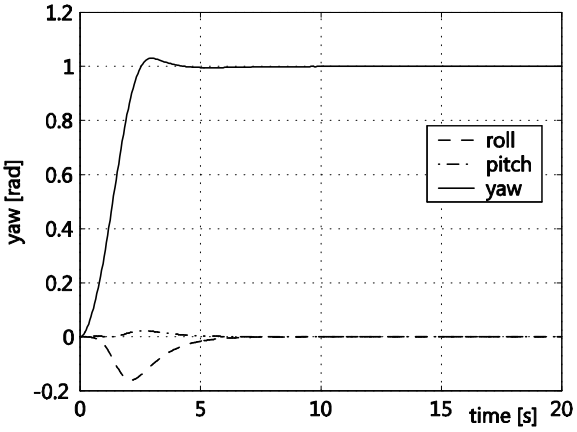


Figure 4: Time history of $\phi(t)$, $\theta(t)$ and $\psi(t)$

The second experiment is to force the ROV to move along a circular trajectory at a constant speed. Consequently, the desired movement of the ROV is defined by $x = R\cos(\omega t)$, $y = R\sin(\omega t)$, $z = const$ and yaw angle $\psi = \pi/2 + \omega t$, in which $R, \omega$ are constant. In this simulation, the radius of the circle has a value of $R = 3$ m. The velocity of the ROV along the trajectory is determined by $V = 0.5$ m/s, with $\omega = 0.5/3$ rad/s.

Figure 5 shows the time history of the coordinates x(t) and y(t). In this figure, the dashed lines represent the desired motions, and the solid lines represent the actual motions. This figure shows that the ROV reaches the desired trajectory after about 10 seconds. The motion of ROV following the circular trajectory is shown in Figure 6.

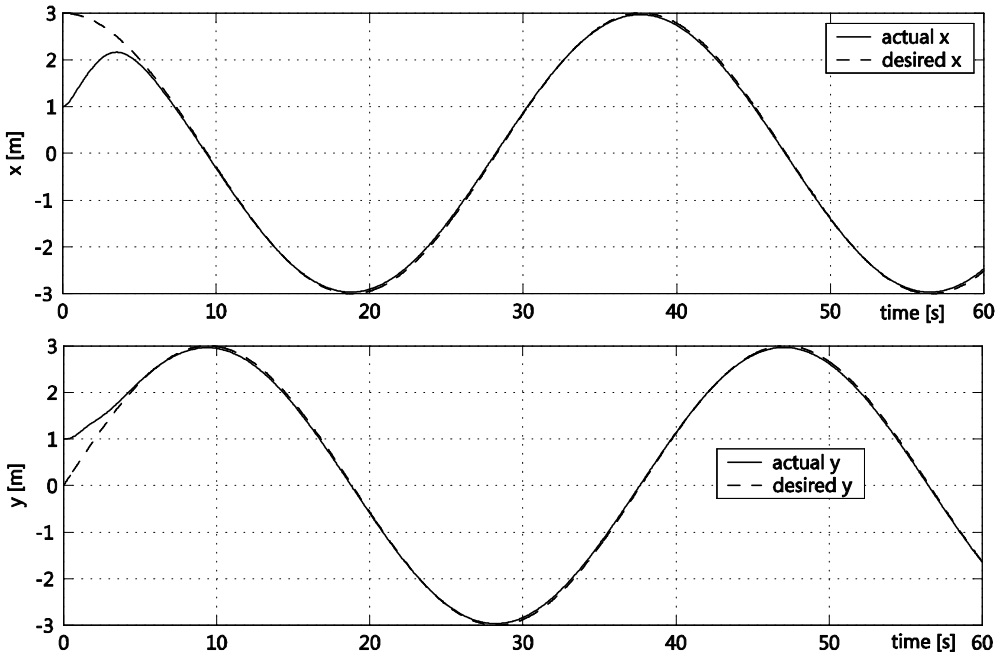


Figure 5: Time history of $x(t)$ and $y(t)$

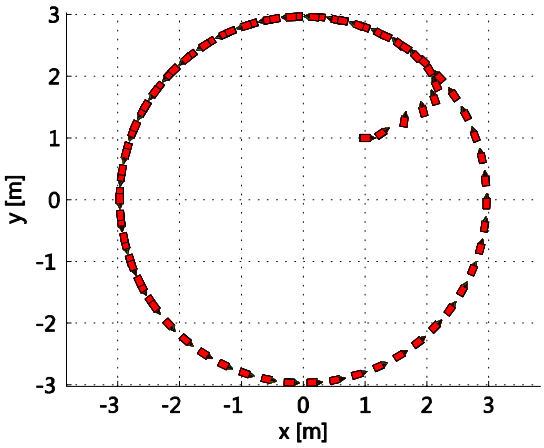


Figure 6: ROV following the circular trajectory

## 6 Conclusion

In this paper we describe the design and implementation of a new adaptive sliding mode controller for dynamic positioning and trajectory tracking of an ROV. The main feature of this design is that it combines the sliding mode control and the adaptive algorithm. This adaptive algorithm is used to estimate the bounds of uncertainties and disturbances. With this controller, prior knowledge about the bounds of system uncertainties and external disturbances is not required. The numerical results in this study show that the controller is able to estimate the bounds of uncertainties and external disturbances online and still provides good performance. The experimental results confirm that the estimated uncertainty bound can successfully adapt the actual one. The proposed approach therefore could reduce the excessive control input when applying the algorithm into both conventional robust control and sliding mode control. The control technique has been finally tested in our simulation case study. The overall sys tem is globally asymptotically stable. Robust control of the position (dynamic positioning) relative to a structure is achieved with the use of adaptive sliding mode controller. A passive arm is used as a position sensor in the region close to an underwater structure. A model ROV has been constructed and used as a test bed for the control systems described.

**References**


Bachmayer, R. and Whitcomb, L.L.: *Toward dynamic thrust control of marine thrusters*. In: Proceedings of the 11th International Symposium on Unmanned Untethered Submersible Technology, pages 407–414, Durham, New Hampshire, USA (August 1999).

Berstecher, R.: *Entwurf eines adaptiven Fuzzy sliding-mode-Reglers*. Dissertation, Duesseldorf : VDI-Verlag (1998).

Cristi, R.; Papoulias, F. A.; and Healey, A. J.: *Adaptive sliding mode control of autonomous underwater vehicles in the dive plane*. IEEE Journal of Oceanic Engineering, 15(3), (1990), 152–159.

Fossen, T.I.: *Guidance and control of ocean vehicles*. John Wiley & Sons, University of Trondheim Norway (1994).

Gao, W. and Hung, J.C.: *Variable structure control of nonlinear systems: A new approach*. IEEE Transactions on Industrial Electronics, 40(1), (1993), 45–55.

Goheen, K.G. and Jefferys, E.R.: *On the adaptive control of remotely operated underwater vehicles*. International Journal of Adaptive Control and Signal Processing, 4, (1990), 287–297.

Hills, S.J. and Yoerger, D.R.: *A nonlinear sliding mode autopilot for unmanned undersea vehicles*. In: OCEANS '94. 'Oceans Engineering for Today's Technology and Tomorrow's Preservation.', vol. 3, pages III/93–III/98, Brest, France (Sep. 1994).

Khalil, H.K.: *Nonlinear systems*. Prentice Hall, Upper Saddle River, NJ, 2 edn. (1996).

Kiriazov, P.; Kreuzer, E.; and Pinto, F.: *Robust feedback stabilization of underwater robotic vehicles*. Robotics and Autonomous Systems, 21, (1997), 415–423.

Kreuzer, E. and Pinto, F.C.: *Controlling the position of a remotely operated underwater vehicle*. Applied Mathematics and Computation, 78, 2-3, (1996), 175–185.

Newman, J.N.: *Marine hydrodynamics*. Cambridge, Mass. [u.a.] : MIT Press, 4 edn. (1982).

Pinto, F.: *Theoretische und experimentelle Untersuchung zur Sensorik und Regelung von Unterwasserfahrzeugen*. VDI Fortschritt-Berichte, Reihe 12, Nr. 292, Duesseldorf: VDI-Verlag (1996).

Slotine, J.J.E.: *Applied nonlinear control*. Prentice Hall, Englewood Cliffs, NJ (1991).

Utkin, V.: *Sliding modes and their application in variable structure control*. Mir, Moscow (1978).

Walchko, K.J.; Novick, D.; and Nechyba, M.C.: *Development of a sliding mode control system with extended Kalman filter estimation for Subjugator*. In: Paper submitted to the Florida Conference on recent advances in robotics, FAU, Dania Beach, FL (May 8-9, 2003).

Whitcomb, L.L. and Yoerger, D.R.: *Development, comparison, and preliminary experimental validation of nonlinear dynamic thruster models*. IEEE Journal of Ocean Engineering, 24, 4, (1999a), 481–494.

Whitcomb, L.L. and Yoerger, D.R.: *Preliminary experiments in model-based thruster control for underwater vehicle positioning*. IEEE Journal of Ocean Engineering, 24, 4, (1999b), 495–506.

Yoerger, D. R. and Slotine, J. E.: *Robust trajectory control of underwater vehicles*. IEEE Journal of Oceanic Engineering, 10(4), (1985), 462–470.


---


*Addresses:* Dr. Nguyen Quang Hoang, Hanoi University of Technology,
Dai Co Viet Str. 1, Hanoi, Vietnam.
Prof. Dr.-Ing.-habil. Edwin Kreuzer, Hamburg University of Technology,
Eissendorfer Strasse 42, D – 21071. Hamburg, Germany
email: hoangnq-dam@mail.hut.edu.vn; kreuzer@tu-harburg.de.